Original Article

Inhibition of pyruvate carboxylase by 1α,25-dihydroxyvitamin D promotes oxidative stress in early breast cancer progression

Tomasz Wilmanski [a], [1], Xuanzhu Zhou [a], [1], Wei Zheng [a], Aparna Shinde [b],
Shawn S. Donkin [a], Michael Wendt [b], John R. Burgess [a], Dorothy Teegarden [a], *

[a] Department of Nutrition Science, Interdepartmental Nutrition Program, Purdue University, West Lafayette, IN, USA
[b] Department of Medicinal Chemistry and Molecular Pharmacology, Purdue University, West Lafayette, IN, USA

ARTICLE INFO

ABSTRACT

Maintaining reductive-oxidative (redox) balance is an essential feature in breast cancer cell survival, with cellular metabolism playing an integral role in maintaining redox balance through its supply of reduced NADPH. In the present studies, the effect of 1,25-dihydroxyvitamin D (1,25(OH)$_2$D) on redox balance was investigated in early stages of breast cancer. Treatment with 1,25(OH)$_2$D promoted oxidative stress in MCF10A-*ras* and MCF10A-*ErbB2* breast epithelial cells, as measured by the decreased ratios of NADPH/NADP+ and reduced to oxidized glutathione (GSH/GSSG). The mRNA and protein expression of the enzyme pyruvate carboxylase (PC) was downregulated with 1,25(OH)$_2$D treatment, suggesting a potential mechanism. Genetic depletion of PC in MCF10A-*ras* cells resulted in a decreased ratio of NADPH/NADP+ and GSH/GSSG, with 1,25(OH)$_2$D treatment having no further effect. Mutation analysis confirmed the presence and functionality of a vitamin D response element in the PC gene promoter region. Collectively, these results provide evidence that 1,25(OH)$_2$D promotes oxidative stress in early breast cancer progression through transcriptional downregulation of PC.

© 2017 Published by Elsevier B.V.

Introduction

Breast cancer incidence in the United States continues to be one of the highest among all cancers. Additionally, approximately 40,610 U.S. women are expected to die from breast cancer in 2017 alone [1]. Therefore, it is imperative to design effective strategies aimed at reducing breast cancer risk as well as prolonging the life of breast cancer patients. Epidemiological evidence suggests that vitamin D may be an effective preventive compound against breast cancer [2]. Both increased sunlight exposure, a prerequisite for endogenous vitamin D synthesis, as well as higher vitamin D intake have been associated with decreased breast cancer risk [3,4]. Although promising, the mechanisms through which vitamin D may prevent breast cancer are unclear and necessitate further investigation.

Vitamin D is biologically activated by two sequential hydroxylation modifications in the liver and kidney, resulting in the generation of the bioactive metabolite 1α,25-dihydroxyvitamin D (1,25(OH)$_2$D). Once synthesized, 1,25(OH)$_2$D binds to the vitamin D receptor (VDR) in target tissues, including breast epithelial cells, and regulates transcription of target genes [5]. Several anticancer effects of 1,25(OH)$_2$D have been reported including inhibition of cell growth and angiogenesis as well as induction of apoptosis [6]. However, the majority of mechanistic studies utilizing 1,25(OH)$_2$D have been conducted in cancer cells at later stages of disease progression. The effect of 1,25(OH)$_2$D on early carcinogenesis that often occurs years before diagnosis has been studied less extensively. Importantly, early prevention in particular may be most effective in decreasing the lifetime risk of breast cancer [7].

Reductive-oxidative (redox) balance is an essential component of cancer cell homeostasis implicated in cell proliferation, progression, and drug resistance [8,9]. Oxidative stress resulting from an imbalance of reactive oxygen species (ROS) and their counteracting antioxidants is mutagenic and thereby promotes cancer progression. However, excess oxidative stress can inhibit cancer cell growth and lead to cell death, highlighting the importance of cancer cells' generation of sufficient reducing potential to maintain an optimal redox balance [10]. To counteract excess ROS, cancer cells often upregulate endogenous antioxidant defenses [11,12].

Recent evidence suggests that even transformed epithelial cells at early stages of cancer progression exhibit decreased oxidative stress and higher antioxidant potential [13]. This reductive environment in early stages of cancer promotes cellular proliferation and survival, and is therefore a promising therapeutic target for cancer prevention.

Intracellular reductive potential is generated through metabolism of nutrients, both glucose and glutamine, which cancer cells metabolize in excess of their energy needs. Glucose may be shunted into the pentose phosphate pathway (PPP), resulting in generation of reduced nicotinamide dinucleotide phosphate (NADPH). NADPH then serves as an electron donor for glutathione reductase-mediated recycling of glutathione (GSH), the most abundant endogenous antioxidant in the cell [14].

In addition to glucose metabolism via the PPP, both glucose and glutamine may contribute to NADPH generation via malic enzyme 1 (ME1). ME1 facilitates the oxidative decarboxylation of malate to pyruvate, generating NADPH in the process. Studies in pancreatic cancer cells demonstrated that the K-ras oncogenic mutation reprograms glutamine metabolism and utilizes ME1 for NADPH generation. The primary enzyme facilitating this metabolic shift in this cell type is glutamic-oxaloacetic transaminase 1 (GOT1). GOT1 generates cytosolic oxaloacetate (OAA) that is further metabolized to malate, hence providing substrates for ME1 [16]. Alternatively, pyruvate derived from glycolysis may also provide substrates for ME1 independent of GOT1 through its metabolism via the mitochondria, as was previously proposed in pancreatic beta cells [17]. Interestingly, ME1 is overexpressed in some cancers [18]. Together, the PPP and ME1 account for majority of NADPH generation in the cell [19].

Previous research in our laboratory demonstrated that $1,25(OH)_2D$ inhibits glucose utilization in MCF10A Harvey-ras (MCF10A-ras) oncogene transfected breast epithelial cells, a model of early breast cancer. Treatment of MCF10A-ras cells with $1,25(OH)_2D$ resulted in decreased glucose metabolism in the glycolytic pathway as well as its flux into the TCA cycle [20]. Additionally, $1,25(OH)_2D$ inhibited glutamine uptake and its downstream flux into the TCA cycle in both MCF10A-ras and MCF10A HER2/neu (MCF10A-ErbB2) overexpressing cells, the latter being one of the most commonly amplified genes in breast cancer [22,23]. Given the importance of glucose and glutamine metabolism in redox balance, and the effect of $1,25(OH)_2D$ on both of these pathways, the purpose of the following studies was to investigate the effect of $1,25(OH)_2D$ on endogenous antioxidant defenses in early stages of breast cancer. It was hypothesized that $1,25(OH)_2D$ acts as a pro-oxidant in transformed breast epithelial cells by reducing metabolic NADPH generation necessary for protection from oxidative stress.

Materials and methods

Chemicals and reagents

Dulbecco's Modified Eagle Medium Nutrient Mixture F-12 (DMEM/F12) media, horse serum, trypsin and penicillin/streptomycin were all obtained from Life Technologies (Rockville, MD). Cholera toxin was purchased from Calbiochem (Darmstadt, Germany) and $1,25(OH)_2D$ was purchased from Biomol (Plymouth Meeting, PA). Protease inhibitor cocktail, insulin, epidermal growth factor, dehydroepiandrosterone (DHEA), UK-5099 and hydrocortisone were purchased from Sigma-Aldrich (St. Louis, MO).

Cell culture

MCF10A-ras and MCF10A-ErbB2 breast epithelial cells were a kind gift from Dr. Michael Kinch, Purdue University. Both cell lines were cultured in standard conditions, as previously described [20]. Treatment with $1,25(OH)_2D$ was conducted in fresh media replaced every 24 h in ethanol (vehicle) at a final concentration <0.1%.

RNA isolation and analysis

RNA isolation and analysis were conducted as described previously [20]. RNA was isolated with TriReagent (Molecular Research Center, Cincinnati, OH) following the manufacturer's instructions. Reverse transcription of total RNA was performed using MMLV reverse transcriptase (Promega, Madison, WI). Brilliant III SYBR Green QPCR Master Mix (Agilent, Santa Clara, CA) was used for real-time quantitative PCR. The mRNA expression was normalized to 18S expression using the $2^{(-delta\ CT)}$ equation and results were expressed as arbitrary units. Primers used are provided in Table 1.

Ribose-5-phosphate quantification

Cells were treated with either vehicle or $1,25(OH)_2D$ for 96 h followed by extraction into lysis buffer and derivatization of cell metabolites with light labeling reagent (6 $M^{12}C_6$-aniline solution). The standard, ribose-5-phosphate (Sigma-Aldrich, St. Louis. MO), was derivatized with heavy labeling reagent (6 $M^{13}C_6$-aniline solution) and mixed 1:1 with the sample. Quantification of ribose-5-phosphate was conducted using 1100 series HPLC (Agilent Technologies, Santa Clare, CA) coupled to an Agilent MSD-TOF (time of flight) mass spectrometer (LC-MS) as described previously [24]. Ribose-5-phosphate concentration was normalized to protein content using Pierce BCA protein assay according to the manufacturer's instructions (Thermo Fisher Scientific, Waltham, MA).

^{13}C-Metabolite flux analysis

^{13}C-glucose flux analysis was conducted as described previously [25]. Briefly, cells were treated for 96 h with either vehicle or $1,25(OH)_2D$. Two hours before harvest, cell media was changed to fresh media containing 50% ^{13}C-[U]-glucose and 50% unlabeled glucose. After incubation, media was collected and stored at $-80\ °C$ until analysis. Samples were processed as described previously [20], and analytes were converted to their t butyldimethylsilyl derivative prior to GC-MS analysis (HP 5973N Mass Selective Detector, Agilent, Palo Alto, CA).

GSH assay

GSH/GSSG ratio quantification was conducted using the Promega GSH/GSSG-Glo™ Assay (Promega, Madison, WI). Cells were plated at a concentration of 3×10^3 cells/well in 96-well plates. After indicated duration of treatment, media was removed and the assay was conducted according to the manufacturer's instructions. Luminescence was measured using the Synergy H1 Multi-mode reader. When investigating the effect of pyruvate carboxylase (PC) knockdown on GSH levels, GSH/GSSG ratio measurements as well as GSSG and total GSH levels were additionally quantified using a colorimetric based assay described previously [26]. GSH/GSSG ratios were calculated using the following equation: GSH/GSSG = [Total GSH-(2 × GSSG)]/GSSG.

NADPH assay

NADPH/NADP+ quantification was conducted using the NADP/NADPH-Glo Assay (Promega, Madison, WI). Cells were plated at 1.4×10^4 cells/well in 24-well plates. After indicated day of treatment, media was removed from the well and cells were washed twice with warm calcium-magnesium free phosphate buffer saline (CMF-PBS). After washing the cells, 200 μL of clear CMF-PBS was added to each well followed by addition of 200 μl of 0.2 N NaOH solution containing 1% dodecyltrimethylammonium bromide (DTAB) (Sigma-Aldrich, St. Louis, MO). Cell lysate was transferred and centrifuged at room temperature for 2 min at 1000 RPM

Table 1
Primers used in QPCR analysis of gene expression.

Genes	Primer information
ME1	Forward: 5′- CGGAACCCTCACCTCAACAA -3′
	Reverse: 5′- GAACCTGGATCTCCTGACTGT -3′
GOT1	Forward: 5′-CAACTGGGATTGACCCAACT-3′
	Reverse: 5′-GGAACAGAAACCGGTGCTT-3′
G6PD	Forward: 5′ -TGCCTTCCATCAGTCGGATACACA-3′
	Reverse: 5′-GCATAGCCCACGATGAAGGTGTTT-3′
hPC	Forward: 5′-ATGTTGCCCACAACTTCAGCAAGC-3′
	Reverse: 5′-AGTTGAGGGAGTCAAACACACGGA-3′
hPC variant 1	Forward: 5′-GACGGCGAGGAGATAGTGTCTG-3′
	Reverse: 5′-GATGGCAATCTCACCTCTGTTGG 3′
hPC variant 2	Forward: 5′-GTGTGGCCTCTCTGGAACTCTG-3′
	Reverse: 5′-GATGGCAATCTCACCTCTGTTGG 3′
hPC variant 3	Forward: 5′-GAGGGAGCTGCCTTCTAGTCTCA-3′
	Reverse: 5′-GATGGCAATCTCACCTCTGTTGG 3′
18S	Forward: 5′-TTAGAGTGTTCAAAGCAGGCCCGA-3′
	Reverse: 5′-TCTTGGCAAATGCTTTCGCTCTGG-3′

to remove cell debris. A 50 μl volume of cell lysate was added to four separate wells of a 96-well plate (two replicates of NADP+ and two of NADPH per sample) and samples were prepared according to the manufacturer's instructions. Luminescence was measured using the Synergy H1 Multi-mode reader and results were expressed as NADPH/NADP+ ratio after subtracting the blank from each sample.

ROS assay

ROS levels were assessed using dichlorofluorescein diacetate (DCFH-DA) (Sigma-Aldrich, St. Louis, MO). DCFH-DA is de-acetylated upon cellular uptake. Once de-acetylated, the probe can be oxidized resulting in a fluorescent signal proportional to the level of intracellular ROS [27]. Cells were plated at a concentration of 3×10^3 cells/well in black clear bottom 96-well plates. After the indicated treatment duration, cell media was aspirated and cells were washed once with CMF-PBS. DCFH-DA stock solution (20 mM) in DMSO was diluted to a final working concentration of 10 μM in CMF-PBS (final concentration DMSO <1%). Cells were incubated in 10 μM DCFH-DA in PBS in the presence or absence of hydrogen peroxide (H_2O_2) (Sigma-Aldrich, St. Louis, MO) and fluorescence was measured after 20 min using a Synergy H1 Multi-Mode reader (ex/em. 485/530). Fluorescence units were normalized to cell viability per well using a 3-(4,5-dimethylthiazol-2-yl)-2,5-diphenyltetrazolium bromide (MTT) assay according to the manufacturer's instructions.

H2O2 challenge assay

Cells were plated in 96-well plates, allowed to attach overnight and treated with either vehicle or 1,25(OH)$_2$D for 72 h. For the last 24 h (96 h total), cells were treated with vehicle or 1,25(OH)$_2$D as well as inhibitors (25 μM UK-5099) and concentrations of H_2O_2 (Sigma-Aldrich, St. Louis, MI). Fresh stock solution of oxaloacetate (OAA) (Sigma Aldrich, St. Louis, MI) was prepared the day of the experiment. The pH of the OAA stock solution was adjusted to 7.4 using 1 N sodium hydroxide solution (NaOH) and sterile filtered. Cell viability was measured at the end of 96 h using an MTT assay according to the manufacturer's instructions.

GOT1 overexpression

MCF10A-*ras* cells were transfected with the pCMV6-Neo or pCMV6-GOT1 (NM_002079) expressing plasmid (Origene Technologies, Rockville, MD) using lipofectamine 2000 and Opti-MEM Reduced Serum Medium (Invitrogen, Carlsbad, CA) according to the manufacturer's instructions. After transfection, transfection media was replaced and cells were treated with media containing vehicle or 1,25(OH)$_2$D (10 nM) for 96 h before analysis.

Doxycycline inducible PC knockdown

Doxycycline (DOX) inducible TRIPZ lentiviral human PC shRNAs were purchased from GE Dharmacon (Lafayette, CO). The shRNA lentiviral plasmids were transfected into HEK293T cells using polyethylenimine to obtain lentiviral particles. MCF10A-*ras* cells were transduced with lentiviral particles for 48 h and stable transfected cells were selected over a span of 14 days using puromycin (5 mg/mL). The target sequence (shRNA sequence) was 5′- TGATGTCTATCACCTTCCC-3′ (ptripz shPC 304). For experiments utilizing 1,25(OH)$_2$D, Dox inducible shPC MCF10A-*ras* cells were treated with vehicle or 1,25(OH)$_2$D for 24 h followed by a 72 h concurrent treatment with vehicle or 1,25(OH)$_2$D ± Dox (10 μg/mL).

Plasmid construction for promoter analysis

A fragment (−575/+23 bp) of the published human distal P2 PC promoter sequence [28] was generated by PCR from genomic DNA of the MCF10A-*ras* cells (Wizard Genomic DNA Purification Kit, Promega, Madison, WI) using primers containing restriction sites (*Kpn*I and *Xho*I) designed from the Homo sapiens pyruvate carboxylase (PC), RefSeqGene on chromosome 11 (NG_008319.1). The sequences of the primers are: forward, 5′-TAATATGGTACCAGTCATGTAACCCGTGTGGC-3′; reverse, 5′-ATAATTCTCGAGTCCACTGACAGAGAACAGCT-3′. The PCR product was first subcloned into the pCR2.1 TA-TOPO cloning vector (Invitrogen, Carlsbad, CA). The sequence of the PCR fragment was confirmed by direct sequencing at the Purdue Genomics Facility. The promoter fragment was then directionally cloned into the promoterless firefly luciferase reporter vector pGL3-basic (Promega, Madison, WI) at the *Kpn*I and *Xho*I sites as the plasmid pGL3-PC(-575)-Luc. The plasmid DNA was prepared using the PureLink HiPure Plasmid Maxiprep Kit (Invitrogen, Carlsbad, CA).

Mutagenesis of the VDRE sequence in PC promoter constructs

Mutations in the putative VDRE sequence, one in the 5′ half-site (potential RXR binding site) and the other in the 3′ half-site (potential VDR binding site), were introduced into the pGL3-PC(-575)-Luc reporter construct using the GeneArt site-directed mutagenesis system (Invitrogen, Carlsbad, CA).

Transient transfection and luciferase assay

MCF10A-*ras* cells were transfected using 1 μl lipofectamine (Invitrogen, Carlsbad, CA) with 800 ng of the promoterless pGL3-Basic-Luc plasmid or the various PC promoter-luciferase reporter constructs, and 8 ng of the *Renilla* luciferase plasmid pRL-null (Promega, Madison, WI). Six hours after transfection, cells were treated with vehicle or 10 nM 1,25(OH)$_2$D containing media for 48 h. Luciferase activity was determined using the Dual-Luciferase Reporter Assay System (Promega, Madison, WI), which was normalized to the *Renilla* luciferase activity.

Statistical analysis

All values are represented as mean ± S.E.M. Comparison of two means was conducted using an Independent Samples *t*-test. Where letters are provided, analysis was conducted using analysis of variance (ANOVA) followed by multiple comparisons of means (Tukey HSD), with $P < 0.05$ considered statistically significant.

Results

1,25(OH)$_2$D increases oxidative stress in early breast cancer progression

NADPH and GSH work in tandem to neutralize ROS and maintain redox balance. More important than total NADPH and GSH pools in measuring oxidative stress is the ratio between the reduced and oxidized forms of these two molecules, as cells may have increased oxidative stress without a change in total concentrations of NADPH and GSH [29]. Therefore, the proportion of reduced to oxidized NADPH and GSH were measured in MCF10A-*ras* cells treated with either vehicle or 1,25(OH)$_2$D (10 nM). The NADPH/NADP+ ratio was decreased by 19% at 72 h and 27% at 96 h (Fig. 1A). Similarly, the ratio of GSH/GSSG was significantly reduced by 37% at 96 h with 1,25(OH)$_2$D treatment (Fig. 1B). In addition, treatment with 1,25(OH)$_2$D for 96 h increased ROS generation by 47% in MCF10A-*ras* cells, further confirming the nutrient's pro-oxidative effect (Fig. 1C). As an additional measure of oxidative stress, cell viability was measured after vehicle or 1,25(OH)$_2$D treatment and a concurrent oxidant (H_2O_2) challenge. Because of the growth inhibitory effect of 1,25(OH)$_2$D (Fig. 1D), cell viability was calculated relative to vehicle treated cells within each H_2O_2 treated group to assess the specific impact of 1,25(OH)$_2$D on H_2O_2 mediated decrease in viable cell number (Fig. 1E). MCF10A-*ras* cells treated with 1,25(OH)$_2$D demonstrated a greater decrease in cell viability in response to an H_2O_2 challenge with increasing doses of H_2O_2, confirming that 1,25(OH)$_2$D acts as a pro-oxidant in transformed breast epithelial cells. To further evaluate whether the effect of 1,25(OH)$_2$D on redox balance extends to cells harboring other oncogenic mutations, the effect of 1,25(OH)$_2$D on redox balance in MCF10A-*ErbB2* breast epithelial cells was investigated. Similar to the results obtained in MCF10A-*ras* cells, both the NADPH/NADP+ as well as the GSH/GSSG ratios were significantly reduced with 1,25(OH)$_2$D treatment at 96 h in MCF10A-*ErbB2* cells by 21% and 17%, respectively (Fig. 2 A&B).

1,25(OH)$_2$D inhibits the pentose phosphate pathway

The PPP is a major contributor of reducing potential through generation of NADPH. Previous studies investigating the effect of 1,25(OH)$_2$D on oxidative stress demonstrated that 1,25(OH)$_2$D upregulates the PPP rate-limiting enzyme glucose-6-phosphate dehydrogenase (G6PD), thereby orchestrating an antioxidant effect in benign prostate epithelial cells [30]. To investigate if 1,25(OH)$_2$D regulates G6PD in the same manner in breast epithelial cells, G6PD mRNA expression was measured in MCF10A-*ras* cells. In contrast to its pro-oxidant effect, G6PD mRNA was upregulated with 1,25(OH)$_2$D treatment at 48 h (Fig. 3A), similar to the effect reported in benign prostate epithelial cells [30]. To further investigate if the PPP is upregulated with 1,25(OH)$_2$D treatment, proportional flux of ^{13}C-glucose into the PPP relative to glycolytic flux was measured after a 96 h treatment with vehicle or 1,25(OH)$_2$D. Flux of glucose into the PPP was significantly downregulated with 1,25(OH)$_2$D by 16% relative to vehicle (Fig. 3B), demonstrating that
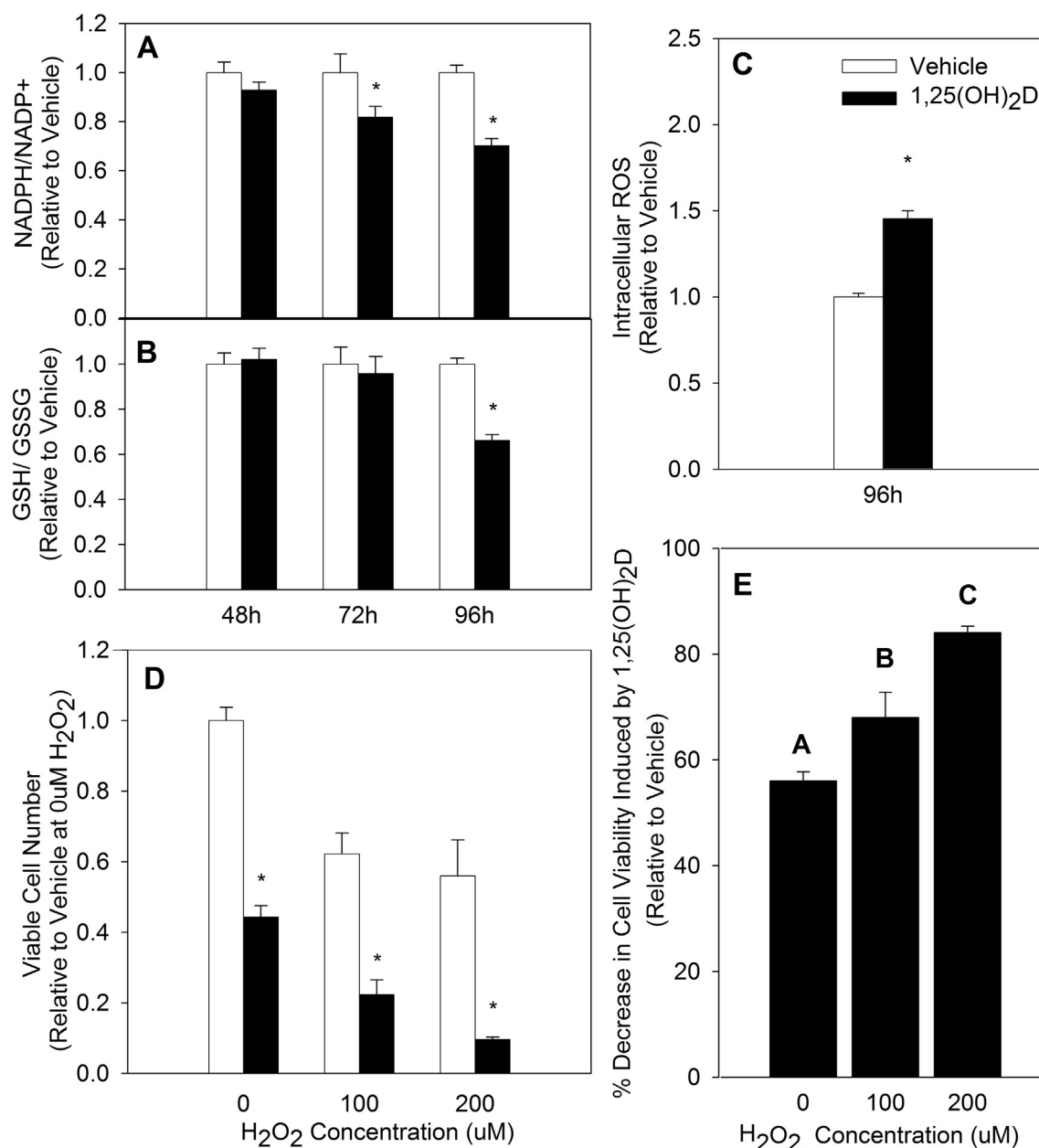
Fig. 1. Impact of 1,25(OH)$_2$D on Oxidative Stress in MCF10A-*ras* Epithelial Cells. MCF10A-ras cells were treated with vehicle or 1,25(OH)$_2$D (10 nM). (A&B) The ratios of reduced to oxidized NADPH and GSH were measured after indicated treatment duration and are expressed relative to vehicle treated results of each time point. (C) Intracellular ROS was measured at time indicated and is expressed relative to vehicle treated cells. (D) Cell viability was quantified after a 24 h challenge with indicated H$_2$O$_2$ concentrations following treatment of cells with vehicle or 1,25(OH)2D for 96 h. (E) The percent decrease in cell viability in 1,25(OH)$_2$D-treated MCF10A-*ras* cells is represented relative to vehicle treated cells at each indicated H$_2$O$_2$ concentration. Values are expressed as mean ± S.E.M. Asterisk indicates significant difference from vehicle ($P < 0.05$). Bars with different letters are significantly different ($P < 0.05$).

1,25(OH)$_2$D inhibits the PPP in MCF10A-*ras* breast epithelial cells despite an upregulation of G6PD. The abundance of intracellular ribose-5-phosphate, the product of PPP that serves as a substrate for nucleoside synthesis, was further investigated utilizing LC-MS. Consistent with a decreased flux of glucose into the PPP, intracellular ribose-5-phosphate concentration was reduced by 25% (Fig. 3C). Having confirmed an inhibition of glucose flux into the PPP by 1,25(OH)$_2$D, the importance of 1,25(OH)$_2$D-mediated inhibition of PPP on oxidative stress was assessed. To this end, DHEA, a non-competitive inhibitor of G6PD, was utilized. DHEA treatment significantly increased intracellular ROS by 18% relative to no DHEA treatment control (Fig. 3D). The effect of 1,25(OH)$_2$D on ROS, however, persisted even in the presence of DHEA (35% and 33%

increase relative to vehicle in the presence and absence of DHEA, respectively). These results suggest that inhibition of PPP does not play a role in 1,25(OH)$_2$D-mediated pro-oxidative effect in MCF10A-*ras* breast epithelial cells.

1,25(OH)$_2$D decreases GOT1 expression

ME1 mediated decarboxylation of malate to pyruvate is a major source of NADPH independent of the PPP. Therefore, mRNA expression of ME1 was measured in both MCF10A-*ras* and MCF10A-*ErbB2* cells treated with vehicle or 1,25(OH)$_2$D. There were no significant differences in ME1 expression in either cell line with 1,25(OH)$_2$D treatment (Fig. 4A). Given that ME1 expression was
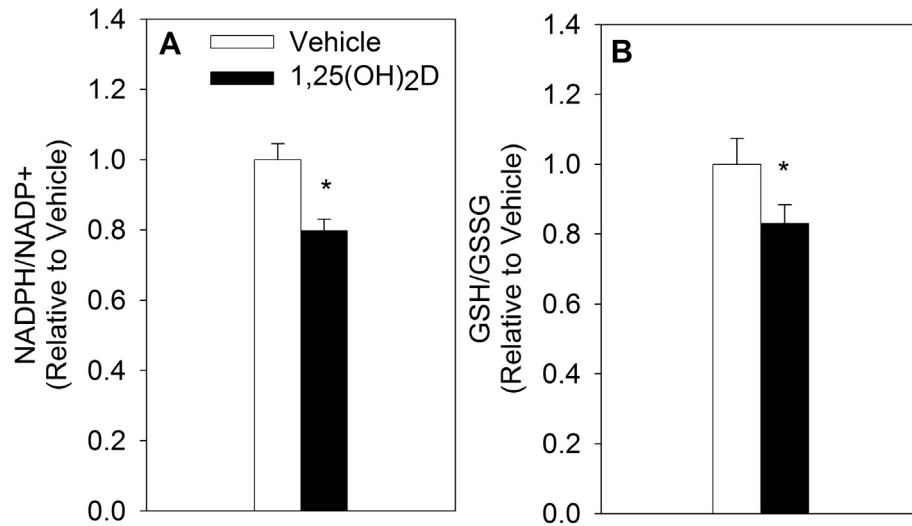
Fig. 2. Impact of 1,25(OH)$_2$D on Oxidative Stress in MCF10A-*ErbB2* Epithelial Cells. MCF10A-*ErbB2* cells were treated with vehicle or 1,25(OH)$_2$D (10 nM) for 96 h and the ratios of reduced to oxidized NADPH and GSH were measured. The results are expressed relative to vehicle treated cells and as mean ± S.E.M. Asterisk (*) indicates significant difference from vehicle ($P < 0.05$) (2-tailed (A) and 1-tailed (B), respectively).
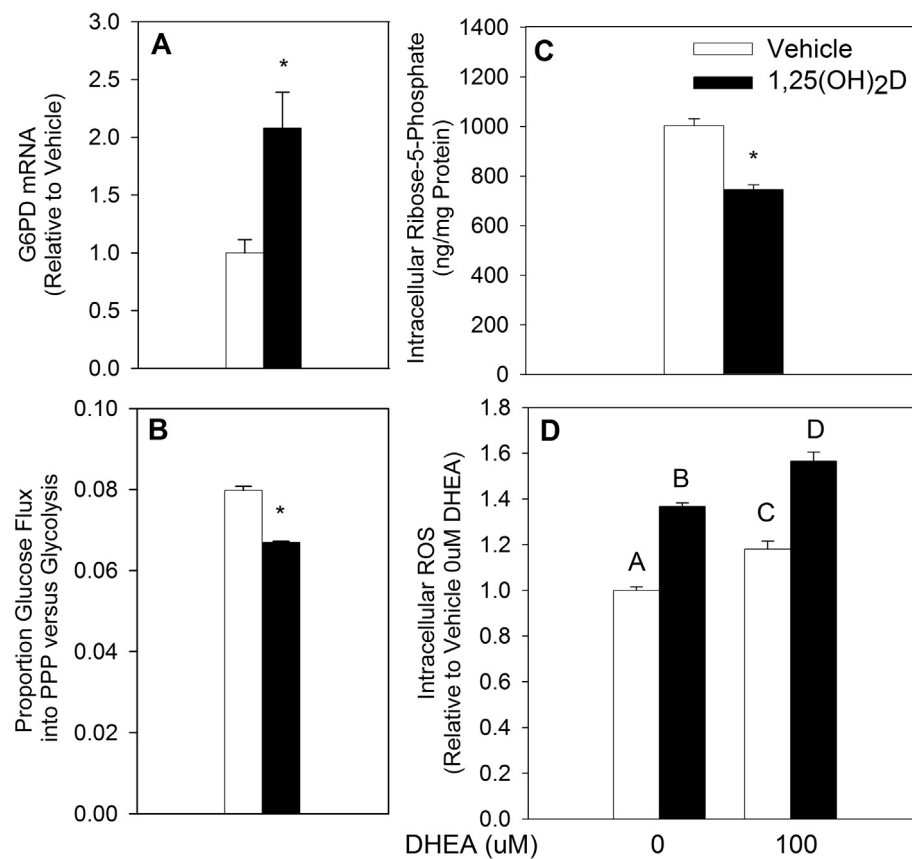
Fig. 3. 1,25(OH)$_2$D-Mediated Regulation of the Pentose Phosphate Pathway. MCF10A-*ras* cells were treated with vehicle or 1,25(OH)$_2$D (10 nM). (A) G6PD mRNA was measured after 48 h of treatment and is expressed relative to vehicle treated cells. (B) Proportion of PPP to glycolytic glucose flux was measured after 96 h of treatment. (C) Intracellular ribose-5-phosphate concentration was measured after 96 h of treatment and is expressed as ng/mg protein. (D) MCF10A-*ras* cells were treated with vehicle or 1,25(OH)$_2$D for 96 h with a concurrent DHEA treatment for the last 24 h. ROS values are expressed relative to vehicle treated cells with no DHEA (0 μM). All values are presented as mean ± S.E.M. Asterisk (*) indicates significant difference from vehicle ($P < 0.05$). Bars with different letters are significantly different ($P < 0.05$).

unchanged with 1,25(OH)$_2$D treatment, metabolic pathways up-stream of ME1 were investigated. Previous studies have implicated GOT1 in maintaining the antioxidant potential of K-*ras* driven pancreatic cancer cells [16]. To investigate 1,25(OH)$_2$D-mediated

impact on GOT1 expression, GOT1 mRNA and protein levels were measured in MCF10A-*ras* cells. Both mRNA and protein levels were significantly decreased with 1,25(OH)$_2$D treatment starting at 48 and 72 h, respectively (Fig. 4B&C). Hypothesizing that 1,25(OH)$_2$D
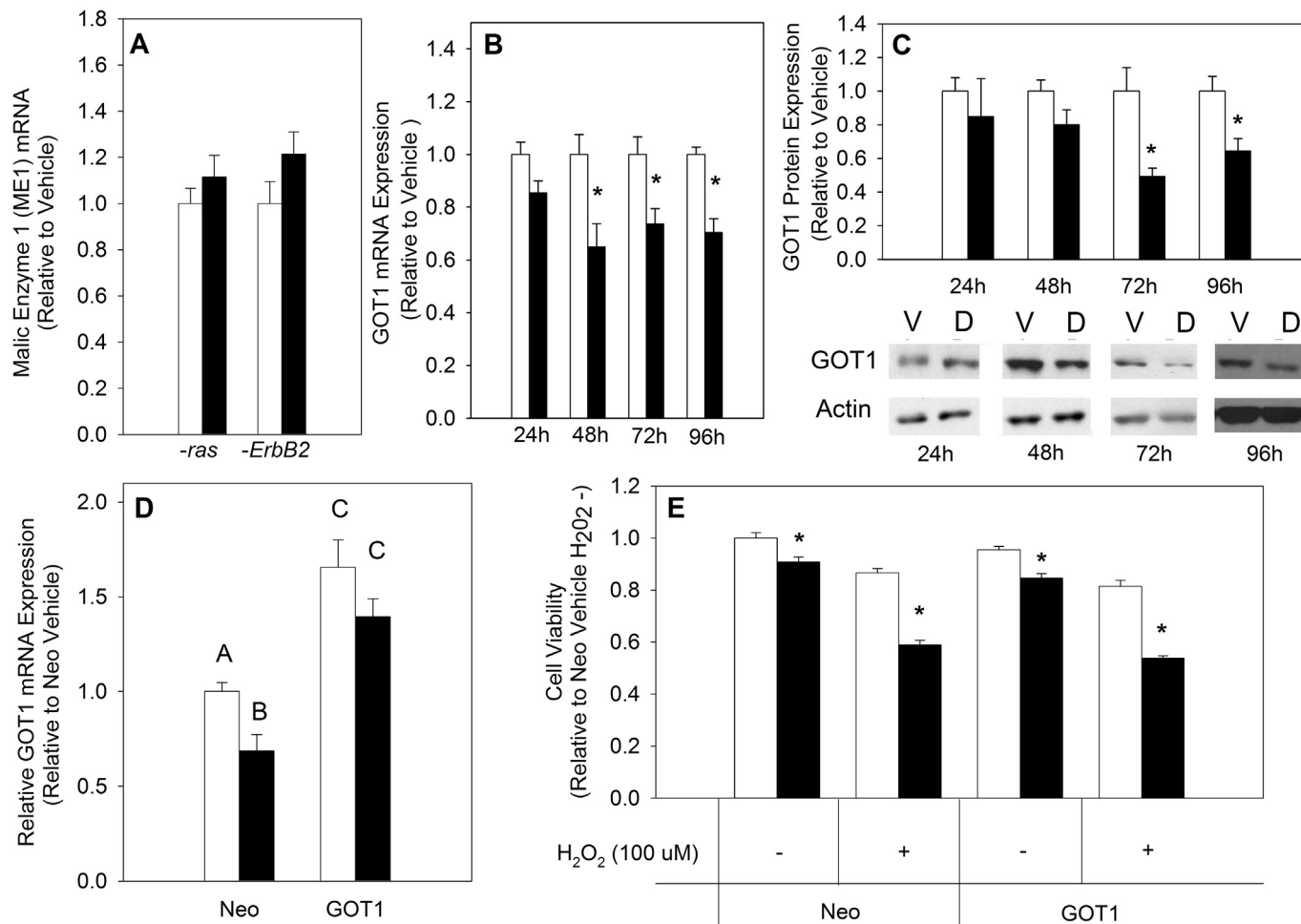
Fig. 4. Effect of 1,25(OH)$_2$D on GOT1 Expression. MCF10A-*ras* cells were treated with vehicle or 1,25(OH)$_2$D (10 nM). (A) ME1 expression was measured after 96 h of treatment using qRT-PCR and normalized to 18S. (B) GOT1 mRNA expression was measured after indicated hours of treatment using qRT-PCR and normalized to 18S. (C) GOT1 protein expression was measured after indicated hours of treatment and normalized to actin. Values are presented relative to vehicle treated cells at each time point and representative images are shown for each time point. (D) GOT1 mRNA expression was measured after cell transfection with a pCMV6-Neo or GOT1 expressing plasmid and 96 h vehicle or 1,25(OH)$_2$D treatment. (E) NEO and GOT1 transfected MCF10A-*ras* cells were treated with vehicle or 1,25(OH)$_2$D for 96 h with a concurrent H$_2$O$_2$ challenge (100 μM) for the last 24 h. Values are expressed as mean ± S.E.M. Asterisk (*) indicates significant difference from vehicle treatment ($P < 0.05$). Bars with different letters are significantly different ($P < 0.05$).

may promote oxidative stress via downregulation of GOT1, an H$_2$O$_2$ assay was performed in the presence or absence of exogenous OAA (2 mM), the product of GOT1 that feeds into ME1-mediated generation of NADPH. OAA in the absence of H$_2$O$_2$ had no effect on cell viability in vehicle or 1,25(OH)$_2$D treated cells (Fig. 5A). However, addition of OAA in the presence of H$_2$O$_2$ rescued MCF10A-*ras* cells from 1,25(OH)$_2$D-mediated effect on H$_2$O$_2$ induced decrease in cell viability (Fig. 5A). This finding was consistent with GOT1 downregulation by 1,25(OH)$_2$D, suggesting that suppression of GOT1 results in decreased OAA levels and hence decreased generation of reduced NADPH. To test this hypothesis, a GOT1 overexpression was achieved through utilizing a pCMV6-plasmid expressing the GOT 1 gene. Successful overexpression of GOT1 was confirmed using qRT-PCR (Fig. 4D). An H$_2$O$_2$ assay was performed to investigate if reversing the effect of 1,25(OH)$_2$D on GOT1 reverses its effect on sensitizing MCF10A-*ras* cells to H$_2$O$_2$ induced decrease in cell viability. Overexpression of GOT1 did not affect the 1,25(OH)$_2$D-mediated decrease in cell viability induced by an H$_2$O$_2$ challenge (Fig. 4E). Therefore, these results suggest that although 1,25(OH)$_2$D downregulates GOT1 mRNA and protein levels, this effect of 1,25(OH)$_2$D is independent of the nutrient's pro-oxidative effect in transformed breast epithelial cells.

1,25(OH)$_2$D promotes oxidative stress through inhibiting mitochondrial pyruvate metabolism

Previous studies in our laboratory demonstrated that 1,25(OH)$_2$D inhibits glucose flux into OAA [20], an upstream metabolite that serves as substrate for malate synthesis and NADPH generation through several pathways. In addition, present studies identified that providing exogenous OAA in the media rescued MCF10A-*ras* cells from 1,25(OH)$_2$D-mediated decrease in cell viability resulting from an H$_2$O$_2$ challenge (Fig. 5A). This finding suggested that 1,25(OH)$_2$D may act as a pro-oxidant due to inhibiting OAA synthesis from glucose via the mitochondria. To test this hypothesis, the impact of 1,25(OH)$_2$D on mitochondrial pyruvate and OAA metabolism in regulating redox balance was investigated in MCF10A-*ras* breast epithelial cells through utilization of the mitochondrial pyruvate carrier (MPC) inhibitor UK-5099. UK-5099 inhibits flux of pyruvate into the mitochondria where pyruvate may be metabolized to either OAA or acetyl-CoA by pyruvate carboxylase (PC) or pyruvate dehydrogenase (PDH), respectively. Co-treatment of vehicle and 1,25(OH)$_2$D treated MCF10A-*ras* cells with UK-5099 resulted in a modest decrease in cell viability (Fig. 5A). However, challenging MCF10A-*ras* cells with
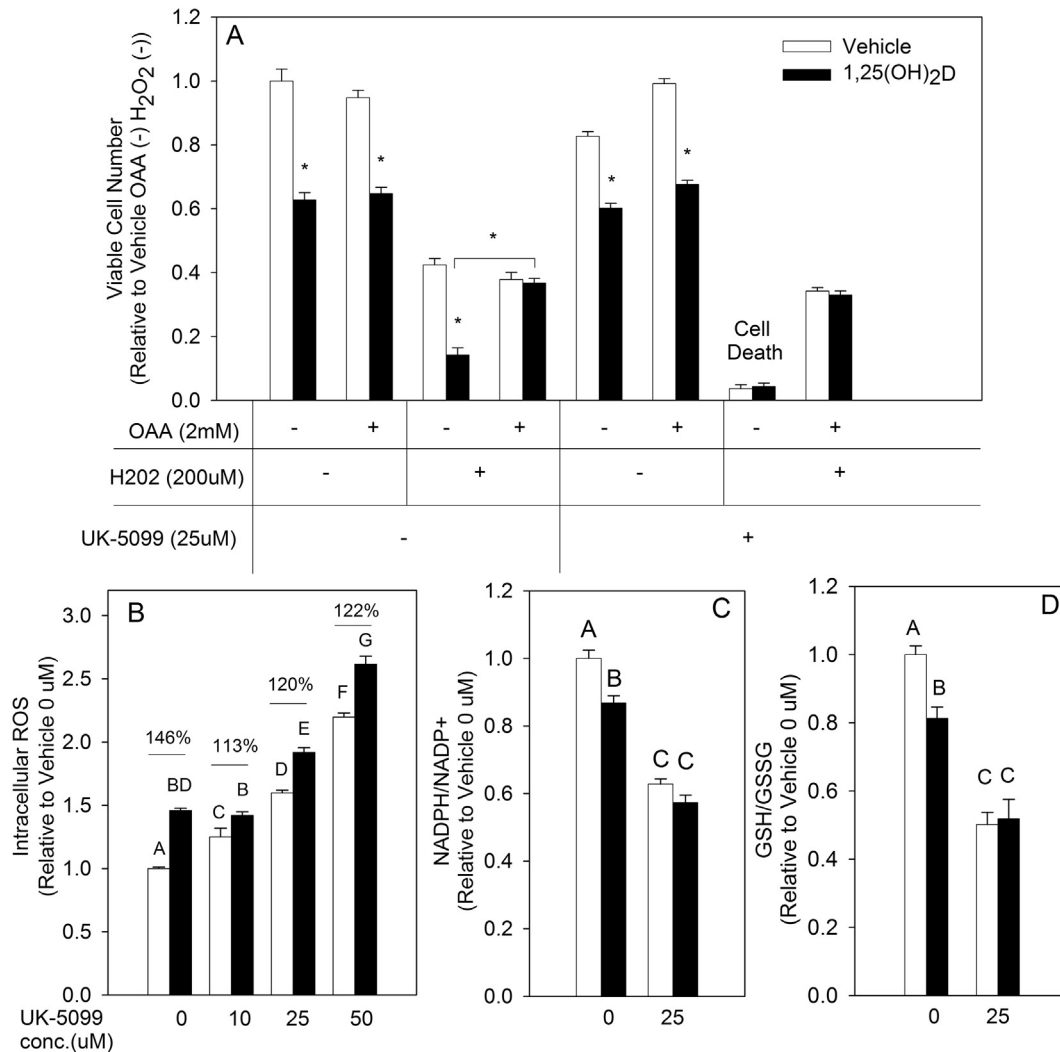
Fig. 5. 1,25(OH)$_2$D-Mediated Effect on Redox Balance Through its Regulation of Mitochondrial Pyruvate Metabolism, (A) MCF10A-*ras* cells were pretreated with vehicle or 1,25(OH)$_2$D (10 nM) for 72 h followed by treatment for an additional 24 h concurrently with H$_2$O$_2$ in the presence or absence of OAA (2 mM) and UK-5099 (25 μM). (B, C&D) Intracellular ROS, NADPH/NADP+ and GSH/GSSG ratios were measured after 96 h of treatment with vehicle or 1,25(OH)$_2$D and a concurrent UK-5099 treatment for the last 24 h. Values are expressed as mean ± S.E.M. Asterisk indicates significant difference from vehicle treatment ($P < 0.05$). Bars with different letters are significantly different ($P < 0.05$).

H$_2$O$_2$ in the presence of UK-5099 resulted in complete cell death of both vehicle and 1,25(OH)$_2$D treated cells (Fig. 5A). Furthermore, OAA rescued both vehicle and 1,25(OH)$_2$D UK-5099 treated cells from an H$_2$O$_2$ challenge, highlighting the importance of mitochondrial pyruvate metabolism and OAA generation in redox balance of MCF10A-*ras* cells. UK-5099 also promoted an increase in ROS levels in a dose dependent manner (Fig. 5B). Treatment with 1,25(OH)$_2$D in the presence of UK-5099 increased ROS only partially compared to its effect in the absence of UK-5099, as shown by a 145% increase at 0 μM versus 113–122% increase in ROS when co-treated with UK-5099 (Fig. 5B). UK-5099 treatment also significantly decreased NADPH/NADP+ (Fig. 5C) and GSH/GSSG (Fig. 5D) ratios in MCF10A-*ras* cells (37% and 50% decrease relative to 0 μM UK-5099, respectively) demonstrating that pyruvate metabolism in the mitochondria is necessary for maintaining redox balance. Treatment with 1,25(OH)$_2$D in the presence of UK-5099 had no additional impact on both the NADPH/NADP+ and GSH/GSSG ratios (Fig. 5C and D), demonstrating that 1,25(OH)$_2$D exerts its pro-oxidant effect through disrupting mitochondrial metabolism of pyruvate.

1,25(OH)$_2$D promotes oxidative stress through inhibiting PC

Previously, 1,25(OH)$_2$D was shown to downregulate PC mRNA and protein expression in metastatic breast cancer cells [31]. PC is a mitochondrial enzyme facilitating the metabolism of pyruvate into OAA. Studies conducted in pancreatic β-cells have implicated PC in sustaining reduced NADPH levels, however its role in maintaining breast epithelial cell redox balance has not yet been explored [32]. To investigate if 1,25(OH)$_2$D downregulates PC expression in early breast cancer progression, PC mRNA and protein levels were measured after vehicle or 1,25(OH)$_2$D treatment of MCF10A-*ras* cells. PC mRNA was significantly downregulated at 24 h while PC protein expression was significantly decreased starting at 48 h of treatment (Fig. 6A and B). Given the importance of PC in supplying mitochondrial OAA and the inhibitory effect of 1,25(OH)$_2$D on PC protein levels, the role of decreased PC in the 1,25(OH)$_2$D mediated effect on oxidative stress was assessed using a stable Dox inducible shPC MCF10A-*ras* cell line. PC knockdown using Dox was confirmed at 96 h of treatment (Fig. 7A and B), with 1,25(OH)$_2$D having no further effect in the presence of Dox. PC knockdown via Dox
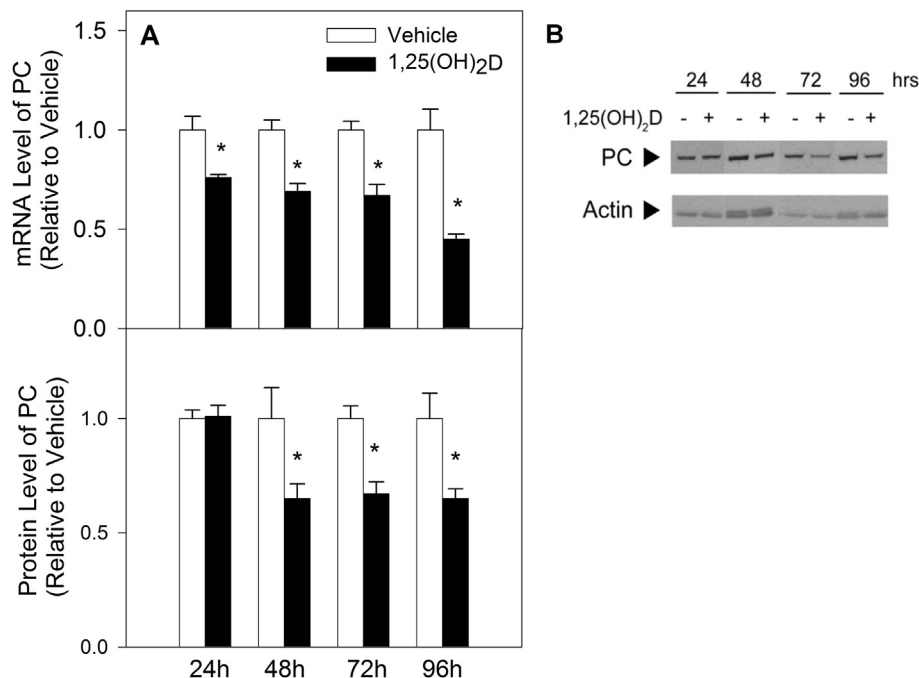
Fig. 6. 1,25(OH)$_2$D-Mediated Effect on PC mRNA and Protein Expression. MCF10A-*ras* cells were treated with vehicle or 1,25(OH)$_2$D (10 nM). (A) PC mRNA expression was measured after indicated hours of treatment using qRT-PCR and normalized to 18S. (B) PC protein expression was measured after indicated hours of treatment and normalized to actin. Values are presented relative to vehicle treated cells at each time point and representative images for each time point are provided. Values are expressed as mean ± S.E.M. (*) Asterisk indicates significant difference from vehicle treatment ($P < 0.05$).

treatment resulted in a significant increase in ROS (Fig. 7C). While the effect of 1,25(OH)$_2$D on ROS persisted even when PC was knocked down, it was only partial to the nutrient's effect in the absence of Dox (Fig. 7C), similar to results obtained when utilizing UK-5099 (Fig. 5B). In addition, PC knockdown resulted in a significant decrease in the NADPH/NADP+ and GSH/GSSG ratios by 61% and 73%, respectively, with 1,25(OH)$_2$D having no further effect (Fig. 7D and E). 1,25(OH)$_2$D treatment further increased GSSG levels in MCF10A-*ras* cells. PC knockdown resulted in significantly higher GSSG levels relative to control cells, and 1,25(OH)$_2$D had no further effect on GSSG levels when PC was knocked down (Fig. 7F). Interestingly, PC knockdown also increased total GSH levels in MCF10A-*ras* cells independent of 1,25(OH)$_2$D treatment (Fig. 7G). This suggests that a high level of PC inhibition promotes a compensatory redox mechanism through increasing synthesis of GSH. Collectively, these results demonstrate that 1,25(OH)$_2$D-mediated downregulation of PC promotes oxidative stress in MCF10A-*ras* breast epithelial cells.

1,25(OH)$_2$D regulation of human PC gene promoter

Because the reduction in PC protein expression at 48 h is preceded by a reduction in mRNA expression at 24 h, the inhibition of PC expression was hypothesized to be orchestrated through direct transcriptional regulation via a classic VDR-mediated genomic action. The promoter of the human PC gene has been characterized in a previous study by Thonpho et al. [28], which indicates that the human PC gene possesses two promoters, the proximal (P1) and the distal (P2) promoter [28]. Three alternative 5′ untranslated region (5′UTR) mRNA variants are produced from the two promoters, with variant 2 transcribed from the proximal promoter while variants 1 and 3 are transcribed from the distal promoter. Previous studies demonstrated that human breast cancer cells express primarily transcript variant 1 [33]. To confirm the same pattern of expression in MCF10A-*ras* cells, real time-PCR analysis of

cDNA was performed using three forward primers that bind to the 5′-untranslated regions (UTR) of variant 1, 2 or 3, with a common reverse primer that binds to exon 1 within the coding region to specifically amplify the three different 5′UTR variants. Consistent with previous studies in human breast epithelial cells, MCF10A-*ras* cells primarily express transcript variant 1 (Fig. 8A). These results confirm that the distal promoter (P2) of the human PC gene controls PC expression in MCF10A-*ras* cells.

To examine whether 1,25(OH)$_2$D regulates the transcriptional activity of the human PC promoter in MCF10A-*ras* cells, a sequence approximately 600 bp upstream (−575/+23 bp) of the transcription start site, which is included in the P2 promoter of PC gene, was inserted into the pGL3-Basic-Luciferase reporter gene plasmid. The pGL3-Basic-Luc plasmid without the promoter or the pGL3-PC(-575)-Luc construct containing the −575 to +23 region of P2 promoter (−575 P2) was co-transfected into MCF10A-*ras* cells with the *Renilla* luciferase plasmid. Cells were treated with vehicle or 1,25(OH)$_2$D for 48 h after transfection. The −575 P2 promoter was functional in inducing luciferase activity by approximately > 300 fold compared to the promoterless pGL3-Basic-Luc plasmid, and 1,25(OH)$_2$D reduced the transcriptional activity of the −575 P2 promoter by 23% compared to vehicle (Fig. 8B), suggesting the presence of a negative VDR regulatory element(s) (VDRE) in this region. These results suggested that 1,25(OH)$_2$D may directly inhibit PC expression at the transcriptional level.

Mutational analysis of the putative VDRE on PC promoter

Analysis of the −575/+23 region of the P2 promoter (−575 P2) revealed a potential VDRE sequence (−403/-389: GGGTGA ATG AATCGA) by homology with the consensus VDRE sequences (Fig. 8D), supporting that 1,25(OH)$_2$D may inhibit PC gene expression at transcriptional level via the VDR. A mutational analysis was carried out to determine whether the suppression of the PC promoter activity by 1,25(OH)$_2$D was mediated through the potential
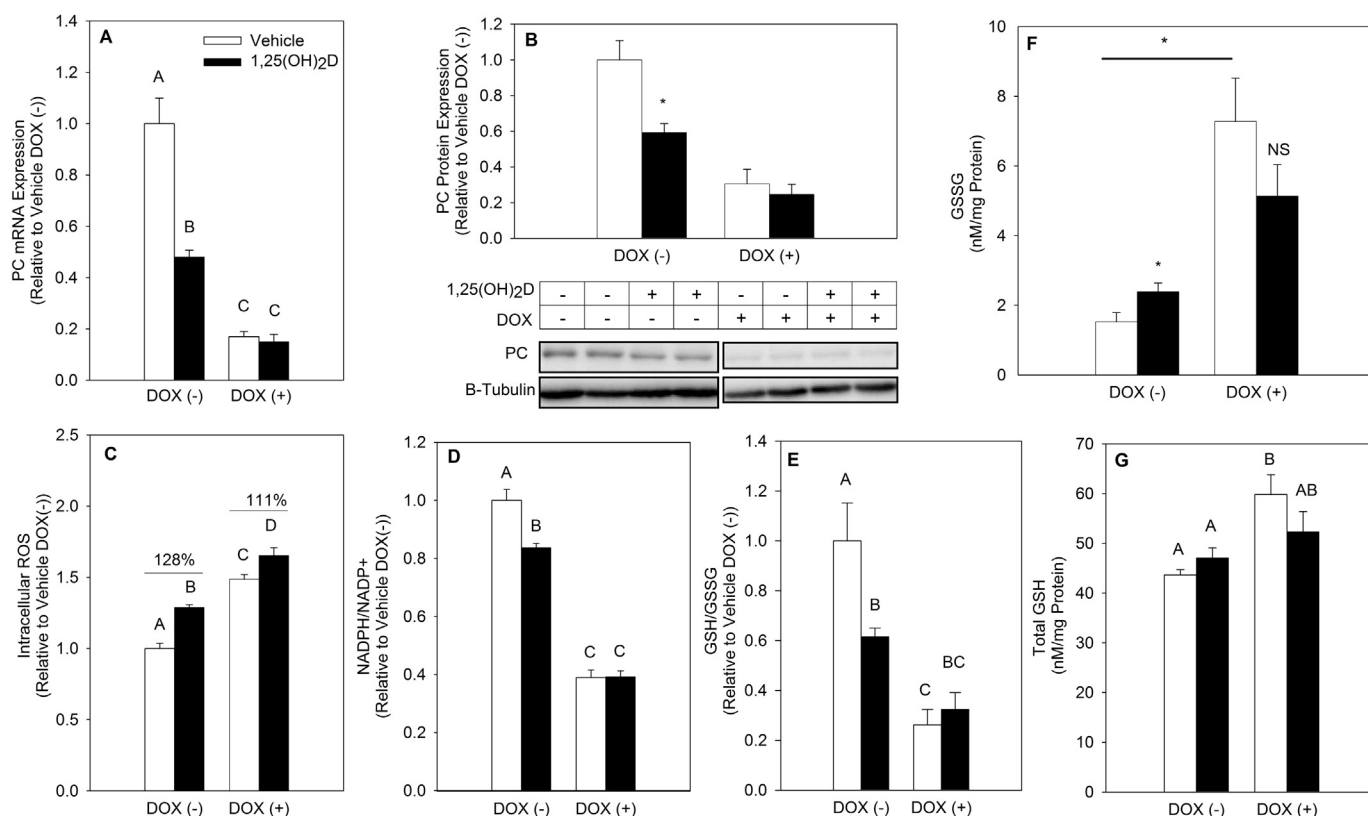
Fig. 7. Effect of 1,25(OH)$_2$D on oxidative stress under PC knockdown. Stably transfected MCF10A-*ras* cells expressing Dox inducible shRNA targeting PC were treated with vehicle or 1,25(OH)$_2$D (10 nM) for 96 h with a concurrent Dox (10 μg/mL) treatment for the last 72 h (A) PC mRNA expression was measured after 96 of treatment using qRT-PCR and normalized to 18S. (B) PC protein expression was measured after 96 h of treatment. Values were normalized to β-tubulin and are expressed relative to vehicle Dox(−) treated cells. Representative blot images are provided. (C–E) ROS levels, NADPH/NADP+ and GSH/GSSG ratios were measured after 96 h of treatment and are expressed relative to vehicle Dox(−) treated group. (F&G) Total GSSG and GSH levels are normalized to protein content. Values are expressed as mean ± S.E.M. (*) Asterisk indicates statistical significance relative to vehicle treated cells. Bars with different letters are statistically significant (*P* < 0.05).

negative VDRE. Site-directed mutagenesis was used to create mutants with base changes in both the 5′ half-site (5′MUT) and 3′ half-site (3′MUT) of the putative VDRE (Fig. 8D) in the pGL3-PC(-575)-Luc reporter construct. Wild-type (WT) PC promoter 2 and the mutant constructs were transfected into the MCF10A-*ras* cells, and 1,25(OH)$_2$D responsiveness was assessed by measuring luciferase reporter activity. As shown in Fig. 8C, 1, 25(OH)$_2$D significantly inhibited the activity of the WT promoter construct, but not the 5′MUT or the 3′MUT promoter constructs. These results suggest that the putative VDRE in the −575 P2 promoter is functional, and both 5′ and 3′ hexameric sequences are required for 1,25(OH)$_2$D suppressor activity via the negative VDRE.

Discussion

Maintaining redox balance is an essential feature of cancer cells implicated in their proliferation, progression and drug resistance [8,9]. In the present studies, the pro-oxidative effect of 1,25(OH)$_2$D is described in transformed breast epithelial cells through its disruption of mitochondrial pyruvate metabolism via transcriptional downregulation of PC. To our knowledge, these are the first studies to demonstrate that metabolic regulation by 1,25(OH)$_2$D facilitates increased ROS and higher oxidative stress in transformed epithelial cells.

The effect of 1,25(OH)$_2$D on oxidative stress may be cell type specific. In contrast to our findings, Bao et al. [30] demonstrated that 1,25(OH)$_2$D acts as an antioxidant in untransformed and benign hyperplasia prostate epithelial cells. The mechanism orchestrating the 1,25(OH)$_2$D-mediated antioxidative effect in these cell types was shown to be dependent on G6PD upregulation. Increased G6PD expression by 1,25(OH)$_2$D in RWPE1 and benign BPH-1 prostate cells facilitated a higher antioxidant potential. Consistent with results reported in prostate epithelial cells, G6PD mRNA in our studies was also upregulated in MCF10A-*ras* epithelial cells with 1,25(OH)$_2$D treatment. However, its upregulation contrasted with a decreased flux of glucose into the PPP (Fig. 3B). Furthermore, 1,25(OH)$_2$D exerted a pro-oxidative effect in MCF10A-*ras* cells even in the presence of DHEA, an uncompetitive inhibitor of G6PD. DHEA itself had a modest effect on ROS in MCF10A-*ras* cells, suggesting that the PPP may not play an essential role in maintaining redox balance in breast epithelial cells at early stages of cancer progression.

Consistent with our present findings, previously published research confirmed a pro-oxidative effect of 1,25(OH)$_2$D in breast cancer cells. For example, treatment of MCF7 cells with 1,25(OH)$_2$D resulted in a decreased ratio of GSH/GSSG, consistent with our findings, as well as increased susceptibility of MCF7 cells to the ROS-generating drug doxorubicin [36,37].

An interesting finding in the present studies was the effect of exogenous OAA on redox balance. OAA rescued MCF10A-*ras* cells from 1,25(OH)$_2$D-mediated increase in sensitivity to a H$_2$O$_2$ challenge. Further, the effect of UK-5099 on oxidative stress was reversed with administration of OAA, suggesting that mitochondrial generation of OAA contributes to maintaining antioxidant defenses in breast epithelial cells.
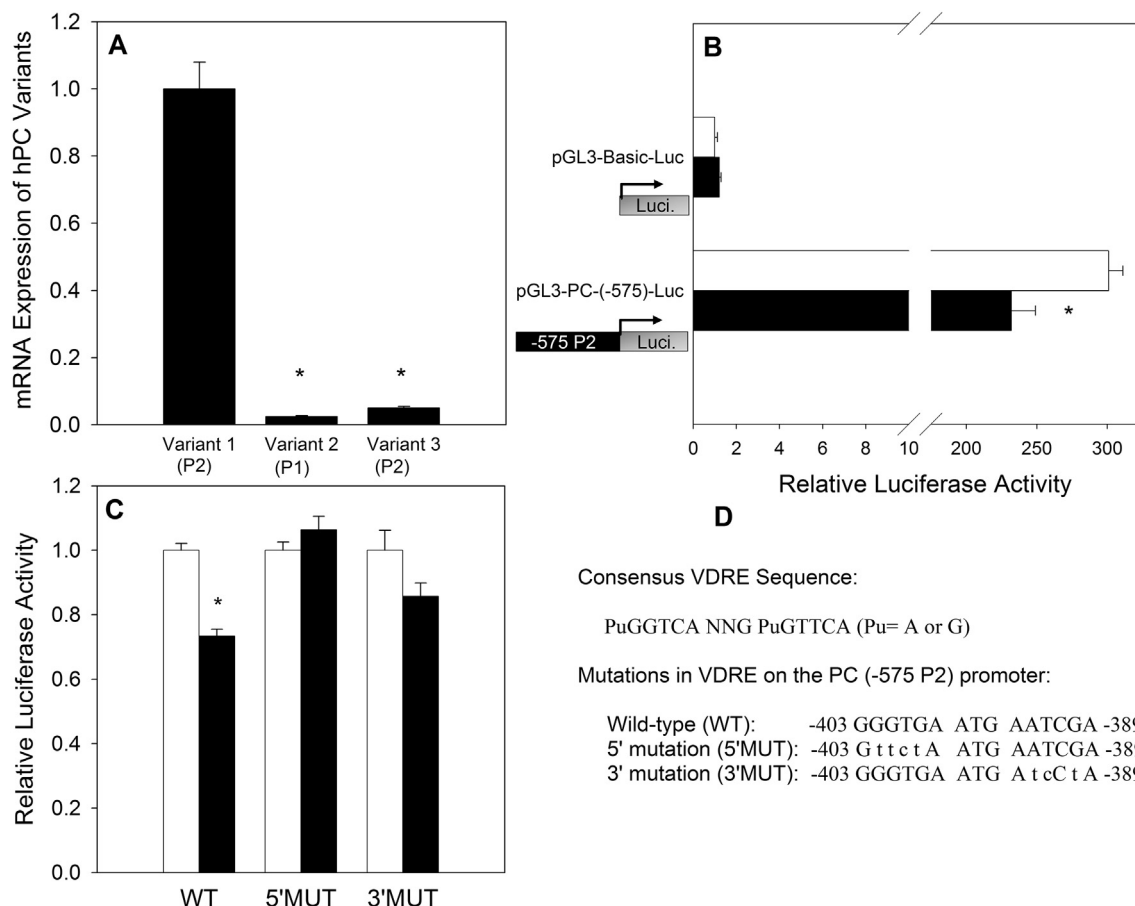
Fig. 8. 1,25(OH)$_2$D-Mediated Transcriptional Regulation of PC. (A) mRNA Expression of three PC variants was measured using qRT-PCR and normalized to 18S. (B) Luciferase activity was measured after 48 h of vehicle or 1,25(OH)$_2$D (10 nM) treatment and is expressed relative to pGL3-Basic-Luc vehicle. (C) Luciferase activity in the wild type (WT), 5′mutation (5′MUT) and 3′mutation (3′MUT) in the VDRE sequence on the P2 promoter after treatment with vehicle or 1,25(OH)$_2$D. Values are expressed relative to vehicle of each promoter construct. (D) Consensus VDRE sequence as well as WT, 5′MUT and 3′MUT sequences are provided. Values are expressed as mean ± S.E.M. (*) Asterisk indicates statistical significance relative to vehicle treated cells ($P < 0.05$).

The role of PC in mediating redox balance has not been an area of interest in cancer research. However, studies investigating the role of PC in pancreatic beta cells demonstrated the essential role of this enzyme in generating NADPH [32]. Similarly, in our studies 1,25(OH)$_2$D mediated transcriptional downregulation of PC decreased the NADPH/NADP+ ratio. These results not only provide a potential mechanism of redox regulation by 1,25(OH)$_2$D, they also highlight the importance of PC and anaplerosis in sustaining redox balance in transformed breast epithelial cells.

An interesting finding in the present study is the characterization of PC as a direct transcriptional target of 1,25(OH)$_2$D. The distal P2 promoter, where the VDRE was identified, regulates transcription of PC in breast epithelial cells as well as pancreatic beta cells [33,38]. PC further plays an important role in glucose stimulated insulin secretion in the latter cell type [32]. Given the direct transcriptional regulation of PC by 1,25(OH)$_2$D via the P2 promoter, the role of 1,25(OH)$_2$D in regulating PC in pancreatic beta cells is an interesting future direction of study.

In summary, our findings present a novel effect of 1,25(OH)$_2$D on cellular metabolism that exerts a pro-oxidative effect in transformed breast epithelial cells through transcriptional downregulation of the anaplerotic enzyme PC via a functional VDRE in the P2 promoter of the PC gene. Further, the results presented in this study demonstrate the importance of PC in maintaining redox balance and suppressing ROS in transformed breast epithelial cells.

Conflict of interest

None.

References

[1] Cancer of the Breast: SEER Stat Fact Sheets, 2014. http://seer.cancer.gov/statfacts/html/breast.html (Accessed 12-01-2015 2015).
[2] C.F. Garland, F.C. Garland, E.D. Gorham, M. Lipkin, H. Newmark, S.B. Mohr, et al., The role of vitamin D in cancer prevention, Am. J. Public Health 96 (2) (2006) 252−261.
[3] S.B. Mohr, C.F. Garland, E.D. Gorham, W.B. Grant, F.C. Garland, Relationship between low ultraviolet B irradiance and higher breast cancer risk in 107 countries, Breast J. 14 (3) (2008) 255−260.
[4] E.M. John, G.G. Schwartz, D.M. Dreon, J. Koo, Vitamin D and breast cancer risk: the NHANES I Epidemiologic follow-up study, 1971-1975 to 1992, Natl. Health Nutr. Exam. Surv. Cancer Epidemiol Biomarkers Prev 8 (5) (1999) 399−406.
[5] G. Zinser, K. Packman, J. Welsh, Vitamin D(3) receptor ablation alters mammary gland morphogenesis, Development 129 (13) (2002) 3067−3076.
[6] J.C. Fleet, M. DeSmet, R. Johnson, Y. Li, Vitamin D and cancer: a review of molecular mechanisms, Biochem. J. 441 (1) (2012) 61−76.
[7] G.A. Colditz, K. Bohlke, Priorities for the primary prevention of breast cancer, CA Cancer J. Clin. 64 (3) (2014) 186−194.
[8] N.S. Brown, R. Bicknell, Hypoxia and oxidative stress in breast cancer. Oxidative stress: its effects on the growth, metastatic potential and response to therapy of breast cancer, Breast Cancer Res. 3 (5) (2001) 323−327.
[9] X.J. Wang, Z. Sun, N.F. Villeneuve, S. Zhang, F. Zhao, Y. Li, et al., Nrf2 enhances resistance of cancer cells to chemotherapeutic drugs, the dark side of Nrf2, Carcinogenesis 29 (6) (2008) 1235−1243.
[10] E. Panieri, M.M. Santoro, ROS homeostasis and metabolism: a dangerous liason in cancer cells, Cell Death Dis. 7 (6) (2016), e2253.

[11] T. Ishimoto, O. Nagano, T. Yae, M. Tamada, T. Motohara, H. Oshima, et al., CD44 variant regulates redox status in cancer cells by stabilizing the xCT subunit of system xc(-) and thereby promotes tumor growth, Cancer Cell 19 (3) (2011) 387—400.

[12] I. Bae, S. Fan, Q. Meng, J.K. Rih, H.J. Kim, H.J. Kang, et al., BRCA1 induces antioxidant gene expression and resistance to oxidative stress, Cancer Res. 64 (21) (2004) 7893—7909.

[13] G.M. DeNicola, F.A. Karreth, T.J. Humpton, A. Gopinathan, C. Wei, K. Frese, et al., Oncogene-induced Nrf2 transcription promotes ROS detoxification and tumorigenesis, Nature 475 (7354) (2011) 106—109.

[14] A. Meister, Selective modification of glutathione metabolism, Science 220 (4596) (1983) 472—477.

[16] J. Son, C.A. Lyssiotis, H. Ying, X. Wang, S. Hua, M. Ligorio, et al., Glutamine supports pancreatic cancer growth through a KRAS-regulated metabolic pathway, Nature 496 (7443) (2013) 101—105.

[17] M.C. Sugden, M.J. Holness, The pyruvate carboxylase-pyruvate dehydrogenase axis in islet pyruvate metabolism: going round in circles? Islets 3 (6) (2011) 302—319.

[18] G. Chakrabarti, Mutant KRAS associated malic enzyme 1 expression is a predictive marker for radiation therapy response in non-small cell lung cancer, Radiat. Oncol. 10 (2015) 145.

[19] J. Fan, J. Ye, J.J. Kamphorst, T. Shlomi, C.B. Thompson, J.D. Rabinowitz, Quantitative flux analysis reveals folate-dependent NADPH production, Nature 510 (7504) (2014) 298—302.

[20] W. Zheng, F. Tayyari, G.A. Gowda, D. Raftery, E.S. McLamore, J. Shi, et al., 1,25-Dihydroxyvitamin D regulation of glucose metabolism in Harvey-ras transformed MCF10A human breast epithelial cells, J. Steroid Biochem. Mol. Biol. 138 (2013) 81—89.

[22] X. Zhou, W. Zheng, G.A. Nagana Gowda, D. Raftery, S.S. Donkin, B. Bequette, et al., 1,25-Dihydroxyvitamin D inhibits glutamine metabolism in Harvey-ras transformed MCF10A human breast epithelial cell, J. Steroid Biochem. Mol. Biol. 163 (2016) 147—156.

[23] E.M. Berns, J.G. Klijn, I.L. van Staveren, H. Portengen, E. Noordegraaf, J.A. Foekens, Prevalence of amplification of the oncogenes c-myc, HER2/neu, and int-2 in one thousand human breast tumours: correlation with steroid receptors, Eur. J. Cancer 28 (2—3) (1992) 697—700.

[24] A. Jannasch, M. Sedlak, J. Adamec, Quantification of pentose phosphate pathway (PPP) metabolites by liquid chromatography-mass spectrometry (LC-MS), Methods Mol. Biol. 708 (2011) 159—171.

[25] W. Zheng, F. Tayyari, G.A. Gowda, D. Raftery, E.S. McLamore, D.M. Porterfield, et al., Altered glucose metabolism in Harvey-ras transformed MCF10A cells, Mol. Carcinog. 54 (2) (February 2015) 111—120.

[26] I. Rahman, A. Kode, S.K. Biswas, Assay for quantitative determination of glutathione and glutathione disulfide levels using enzymatic recycling method, Nat. Protoc. 1 (6) (2006) 3159—3165.

[27] B. Kalyanaraman, V. Darley-Usmar, K.J. Davies, P.A. Dennery, H.J. Forman, M.B. Grisham, et al., Measuring reactive oxygen and nitrogen species with fluorescent probes: challenges and limitations, Free Radic. Biol. Med. 52 (1) (2012) 1—6.

[28] A. Thonpho, P. Rojvirat, S. Jitrapakdee, M.J. MacDonald, Characterization of the distal promoter of the human pyruvate carboxylase gene in pancreatic beta cells, PLoS One 8 (1) (2013), e55139.

[29] F.Q. Schafer, G.R. Buettner, Redox environment of the cell as viewed through the redox state of the glutathione disulfide/glutathione couple, Free Radic. Biol. Med. 30 (11) (2001) 1191—1212.

[30] B.Y. Bao, H.J. Ting, J.W. Hsu, Y.F. Lee, Protective role of 1 alpha, 25-dihydroxyvitamin D3 against oxidative stress in nonmalignant human prostate epithelial cells, Int. J. Cancer 122 (12) (2008) 2699—2706.

[31] T. Wilmanski, K. Buhman, S.S. Donkin, J.R. Burgess, D. Teegarden, 1α,25-dihydroxyvitamin D inhibits de novo fatty acid synthesis and lipid accumulation in metastatic breast cancer cells through down-regulation of pyruvate carboxylase, J. Nutr. Biochem. 40 (2017) 194—200.

[32] X. Li, K.K. Cheng, Z. Liu, J.K. Yang, B. Wang, X. Jiang, et al., The MDM2-p53-pyruvate carboxylase signalling axis couples mitochondrial metabolism to glucose-stimulated insulin secretion in pancreatic β-cells, Nat. Commun. 7 (2016), 11740.

[33] P. Phannasil, C. Thuwajit, M. Warnnissorn, J.C. Wallace, M.J. MacDonald, S. Jitrapakdee, Pyruvate carboxylase is up-regulated in breast cancer and essential to support growth and invasion of MDA-MB-231 cells, PLoS One 10 (6) (2015), e0129848.

[36] R. Koren, I. Hadari-Naor, E. Zuck, C. Rotem, U.A. Liberman, A. Ravid, Vitamin D is a prooxidant in breast cancer cells, Cancer Res. 61 (4) (2001) 1439—1444.

[37] A. Ravid, D. Rocker, A. Machlenkin, C. Rotem, A. Hochman, G. Kessler-Icekson, et al., 1,25-Dihydroxyvitamin D3 enhances the susceptibility of breast cancer cells to doxorubicin-induced oxidative damage, Cancer Res. 59 (4) (1999) 862—867.

[38] S. Jitrapakdee, M. St Maurice, I. Rayment, W.W. Cleland, J.C. Wallace, P.V. Attwood, Structure, mechanism and regulation of pyruvate carboxylase, Biochem. J. 413 (3) (2008) 369—387.